Acta Cryst E CRYSTALLOGRAPHIC COMMUNICATIONS

ISSN 2056-9890

Crystal structure determination, Hirshfeld surface analysis and energy frameworks of 6-phenylsulfonyl-6*H*-thieno[3,2-*c*]carbazole

U. Mohamooda Sumaya,[a] E. Sankar,[b] K. Arasambattu MohanaKrishnan,[b] K. Biruntha[a] and G. Usha[c]*

[a]Department of Physics, Bharathi Women's College (A), Chennai-108, Tamilnadu, India, [b]Department of organic Chemistry, University of Madras, Chennai-25, Tamilnadu, India, and [c]PG and Research Department of Physics, Queen Mary's College (A), Chennai-4, Tamilnadu, India. *Correspondence e-mail: guqmc@yahoo.com

Received 16 April 2018
Accepted 30 May 2018

Edited by L. Fabian, University of East Anglia, England

Keywords: crystal structure; carbazole; Hirshfeld surface analysis; two-dimensional fingerprint plot; energy frameworks.

CCDC reference: 1825258

Supporting information: this article has supporting information at journals.iucr.org/e

In the title compound, $C_{20}H_{13}NO_2S_2$, the carbazole ring system forms a dihedral angle of 89.08 (1)° with the sulfonyl-substituted phenyl ring. Intramolecular C—H···O hydrogen bonds involving the sulfone O atoms and the carbazole moiety result in two $S(6)$ rings. In the crystal, molecules are linked *via* pairs of C—H···O hydrogen bonds forming inversion dimers with an $R_2^2(12)$ graph-set motif. Analysis of the Hirshfeld surfaces and two-dimensional fingerprint plots was used to explore the distribution of weak intermolecular interactions in the crystal structure.

1. Chemical context

Carbazole derivatives are among the most important and highly exploited heterocyclic compounds in the field of medicinal chemistry. They have been attractive to researchers because of their broad spectrum of biological activities, such as anti-oxidative (Tachibana *et al.*, 2001), antitumor (Itoigawa *et al.*, 2000), anti-inflammatory and antimutagenic (Ramsewak *et al.*, 1999), antibiotic, antifungal and cytotoxic (Chakraborty *et al.*, 1965, 1978), pim kinase inhibitory (Giraud *et al.*, 2014), antimicrobial (Gu *et al.*, 2014) and anti-Alzheimer (Thiratmatrakul *et al.*, 2014). Carbazole derivatives are also used as precursor compounds for the synthesis of pyridocarbazole alkaloids (Karmakar *et al.*, 1991).

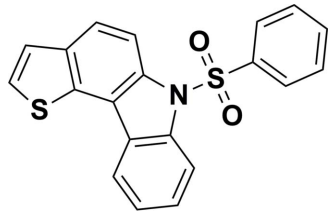

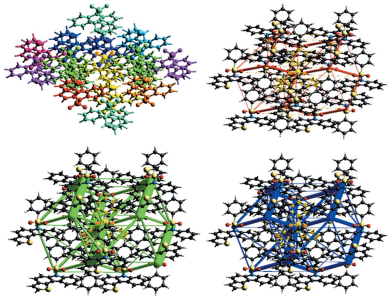

2. Structural commentary

The molecular structure of the title compound is illustrated in Fig.1. The title compound comprises a carbazole ring system, which is attached to a phenyl sulfonyl ring and a thiopene ring. The carbazole ring system forms a dihedral angle of 89.08 (1)° with the sulfonyl-substituted phenyl ring. The tetrahedral configuration is distorted around the atom S2. The increase in the O2—S2—O1 angle [120.14 (9)°], with a simultaneous

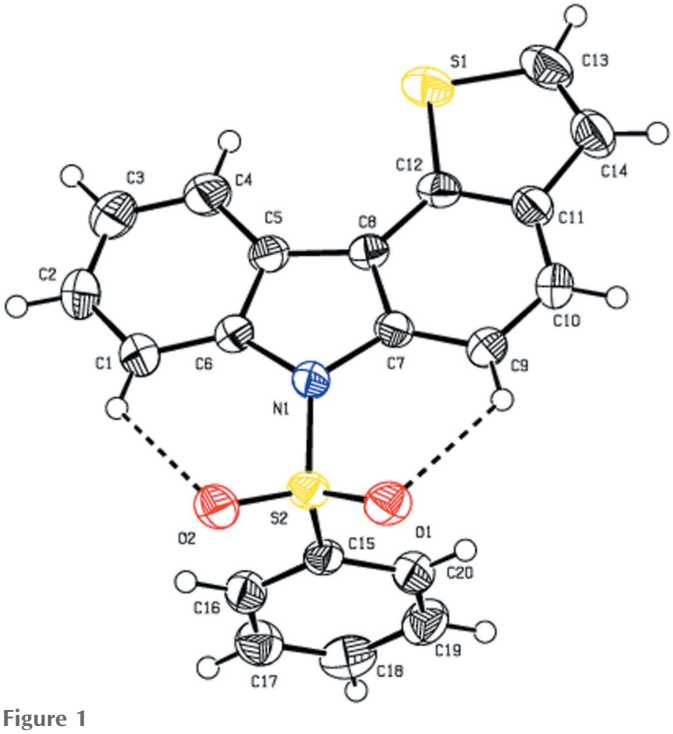

Figure 1
The molecular structure of the title compound with the atom labelling. Displacement ellipsoids are drawn at the 50% probability level. Dashed lines indicate the intramolecular C—H···O hydrogen bonds, which generate *S*(6) ring motifs.

decrease in the N1—S2—C15 angle [104.96 (9)°] from the ideal tetrahedral value (109.5°) are attributed to the Thorpe–Ingold effect (Bassindale, 1984). The N1—C6 [1.428 (2) Å] and N1—C7 [1.429 (2) Å] bond lengths in the molecule are longer than the mean Nsp^2—Csp^2 bond length value of 1.355 (14) Å (Allen *et al.*, 1987; Groom *et al.*, 2016). The elongation observed may be due to the electron-withdrawing character of the phenylsulfonyl group. The molecular structure is stabilized by C1—H1···O2 and C9—H9···O1 intramolecular interactions involving the sulfone oxygen atoms, which generate two *S*(6) ring motifs (Fig. 1).

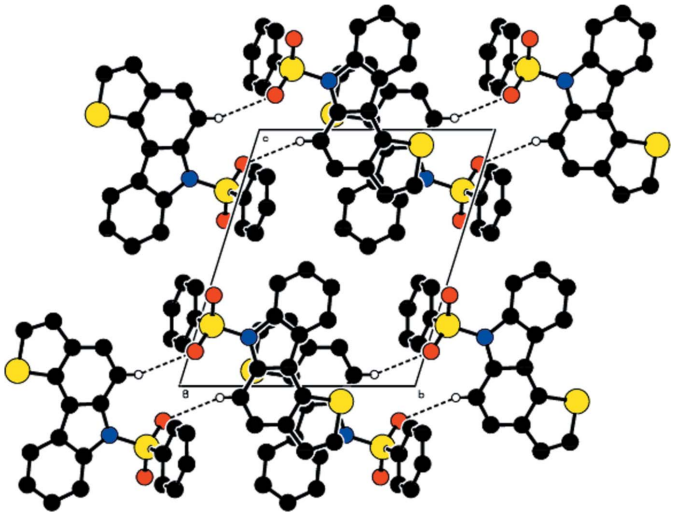

Figure 2
The crystal packing of the title compound, viewed along the *a* axis. Dashed lines indicate intermolecular hydrogen bonds. For clarity, only the H atoms involved in these interactions have been included.

Table 1
Hydrogen-bond geometry (Å, °).

*Cg*5 is the centroid of the C15–C20 ring.

D—H···*A*	*D*—H	H···*A*	*D*···*A*	*D*—H···*A*
C1—H1···O2	0.93	2.34	2.935 (3)	121
C1—H1···O2^{i}	0.93	2.62	3.443 (3)	148
C9—H9···O1	0.93	2.35	2.949 (3)	122
C9—H9···O1^{ii}	0.93	2.57	3.382 (2)	146
C13—H13···*Cg*5^{iii}	0.93	2.82	3.604 (2)	143

Symmetry codes: (i) $-x+1, -y, -z+1$; (ii) $-x+1, -y, -z$; (iii) $-x, -y+1, -z$.

3. Supramolecular features

In the crystal packing (Fig. 2), the molecules are linked *via* pairs of C—H···O hydrogen bonds (Table 1), forming inversion dimers with an $R_2^2(12)$ graph-set motif. Each molecule is involved in the formation of two dimers that propagate as a ribbon in the *c*-axis direction.

4. Hirshfeld surface analysis, interaction energies and energy frameworks

In order to investigate the weak intermolecular interactions in the crystal, the Hirshfeld surfaces (d_{norm}, curvedness and shape index) and 2D fingerprint plots were generated using *CrystalExplorer 17.5* (Turner *et al.*, 2017). The d_{norm} mapping uses the normalized functions of d_i and d_e (Fig. 3*a*), with white, red and blue coloured surfaces where d_i (*x* axis) and d_e (*y* axis) are the closest internal and external distances from a given point on the Hirshfeld surface to the nearest atom. The white surface indicates those contacts with distances equal to the sum of van der Waals (vdW) radii, red indicates shorter

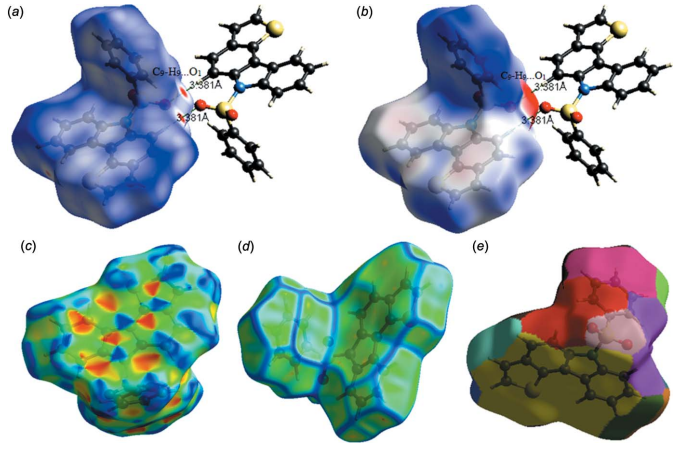

Figure 3
Hirshfeld surfaces for visualizing the intermolecular contacts of the title compound: (*a*) d_{norm} highlighting the regions of C—H···O hydrogen bonds, (*b*) electrostatic potential, (*c*) shape index, (*d*) curvedness and (*e*) fragment patches.

Table 2
Scale factors for benchmarked energy model.

Energy model	k_{elec}	k_{pol}	$k_{energy\text{-}dispersive}$	k_{rep}
CE-B3LYP···B3LYP/6–31G(d,p) electron densities	1.057	0.740	0.871	0.618

contacts (< vdW radii) and blue longer contacts (> vdW radii). The electrostatic potential was also mapped on the Hirshfeld surface using a STO-3G basis set and the Hartee–Fock level of theory (Spackman *et al.*, 2008; Jayatilaka *et al.*, 2005). The C—H···O hydrogen-bond donors and acceptors are shown as blue and red regions around the atoms corresponding to positive and negative electrostatic potentials, respectively (Fig. 3*b*). The presence of π–π stacking interactions is indicated by red and blue triangles on the shape-index surface (Fig. 3*c*). Areas on the Hirshfeld surface with high curvedness tend to divide the surface into contact patches with each neighbouring molecule. The coordination number in the crystal is defined by the curvedness of the Hirshfeld surface (Fig. 3*d*). The nearest neighbour coordination environment of a molecule is identified from the colour patches on the Hirshfeld surface depending on their closeness to adjacent molecules (Fig. 3*e*).

Two-dimensional fingerprint plots showing the occurrence of all intermolecular contacts (McKinnon *et al.*, 2007) are presented in Fig. 4*a*. The fingerprint plot of H···H contacts, which represent the largest contribution to the Hirshfeld surfaces (40%), shows a distinct pattern with a minimum value of $d_e = d_i \simeq 1.2$ Å (Fig. 4*b*). The C···H/H···C interactions appear as the next largest region of the fingerprint plot, highly concentrated at the edges, having almost the same $d_e + d_i \simeq 2.7$ Å (Fig. 4*c*), with an overall Hirshfeld surface contribution of 24.1%. The O···H/H···O interactions on the fingerprint

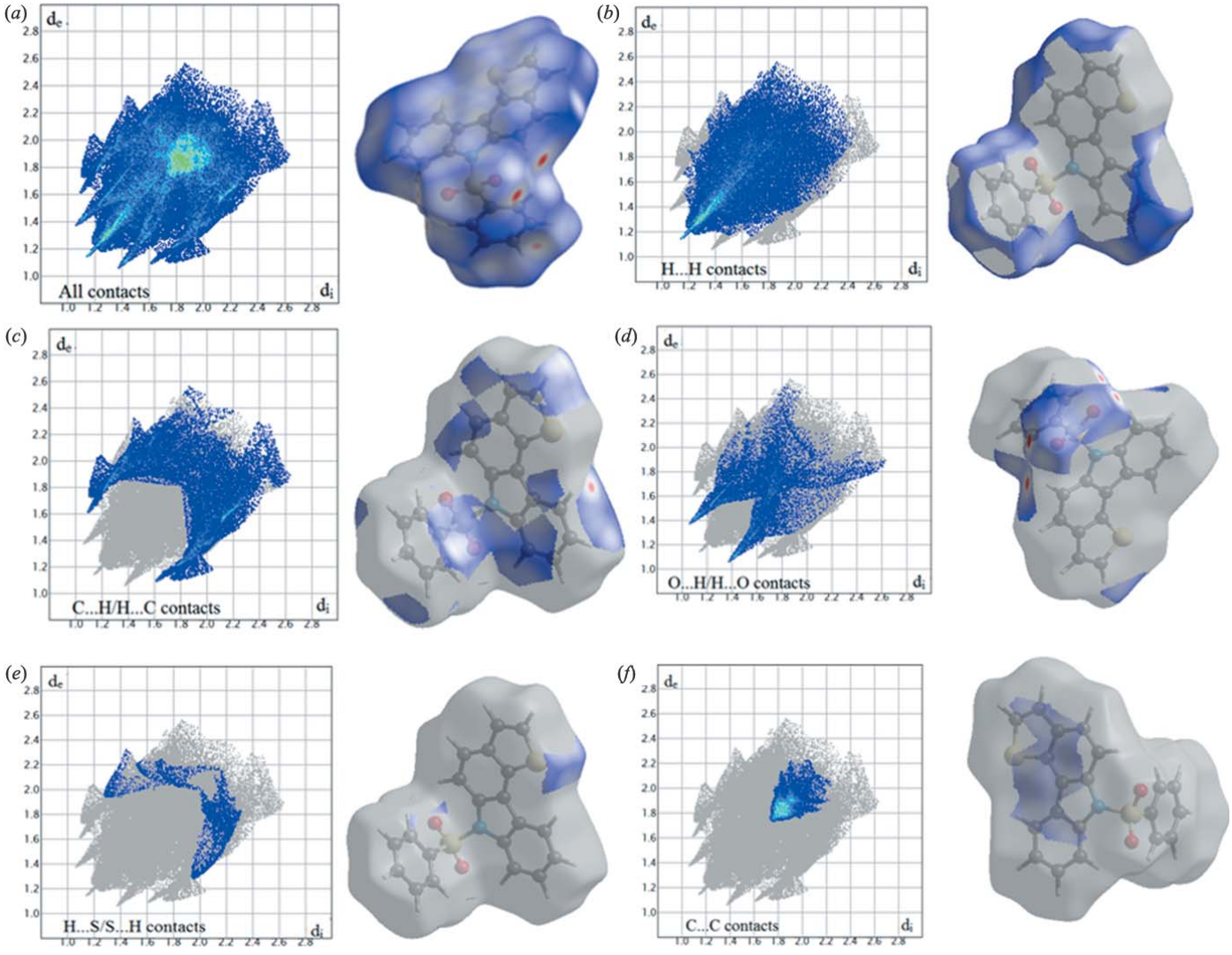

Figure 4
Two-dimensional fingerprint plots for the title compound showing the contributions of different types of interactions: (*a*) all intermolecular contacts, (*b*) H···H contacts, (*c*) C···H/H···C contacts, (*d*) O···H/H···O contacts, (*e*) H···S/S···H contacts and (*f*) C···C contacts. The outline of the the full fingerprint is shown in gray. Surfaces to the right highlight the relevant surface patches associated with the specific contact type and are coloured as d_{norm}.

Table 3
Interaction energies (kJ mol^{-1}) between a reference molecule and its neighbours.

N is the number of equivalent neighbours, *R* is the distance between molecular centroids (mean atomic position) in Å. The colours identify molecules in Fig. 5*a*, with the reference molecule shown in grey.

Colour	*N*	symmetry	*R*	E_{elec}	E_{pol}	$E_{energy\text{-}dispersive}$	E_{rep}	E_{total}
Red	1	inversion	9.29	−3.7	−1.5	−27.5	14.6	−20.0
Orange	1	inversion	8.65	0.9	−1.4	−23.3	10.3	−14.0
Yellow	1	inversion	6.18	−12.2	−2.6	−83.1	54.3	−53.7
Green	2	translation	12.53	1.7	−0.5	−7.3	2.4	−3.4
Lime	2	translation	9.88	−2.4	−0.6	−19.5	14.0	−11.3
Aqua	2	translation	7.65	−4.5	−2.1	−12.1	5.4	−13.5
Cyan	1	inversion	7.79	−17.5	−4.8	−23.5	16.7	−32.2
Blue	1	inversion	8.76	−19.3	−5.0	−26.9	22.3	−33.8
Indigo	1	inversion	5.84	−11.7	−2.7	−87.7	51.5	−58.9
Purple	2	translation	11.22	1.9	−0.4	−6.9	3.6	−2.0
Pink	1	inversion	10.79	−2.6	−0.4	−8.1	2.1	−8.8

plot, which contribute 15.1% of the total Hirshfeld surface with $d_e + d_i \simeq 2.5$ Å (Fig. 4*d*), are shown as two symmetrical narrow pointed wings. The H···S/S···H interactions cover only 3.5% (Fig. 4*e*) of the surface. The C···C contacts, which are the measure of π–π stacking interactions, occupy 8.7% of the Hirshfeld surface and appear as a unique triangle at $d_e = d_i \simeq 1.8$ Å (Fig. 4*f*). These are the weak interactions that contribute the most to the packing of the title compound.

The interaction energy between the molecules is expressed in terms of four components: electrostatic, polarization, dispersion and exchange repulsion. These energies were obtained using monomer wavefunctions calculated at the B3LYP/6-31G(d,p) level. The total interaction energy, which is the sum of scaled components, was calculated for a 3.8 Å radius cluster of molecules around the selected molecule (Fig. 5*a*). The scale factors used in the CE-B3LYP bench-

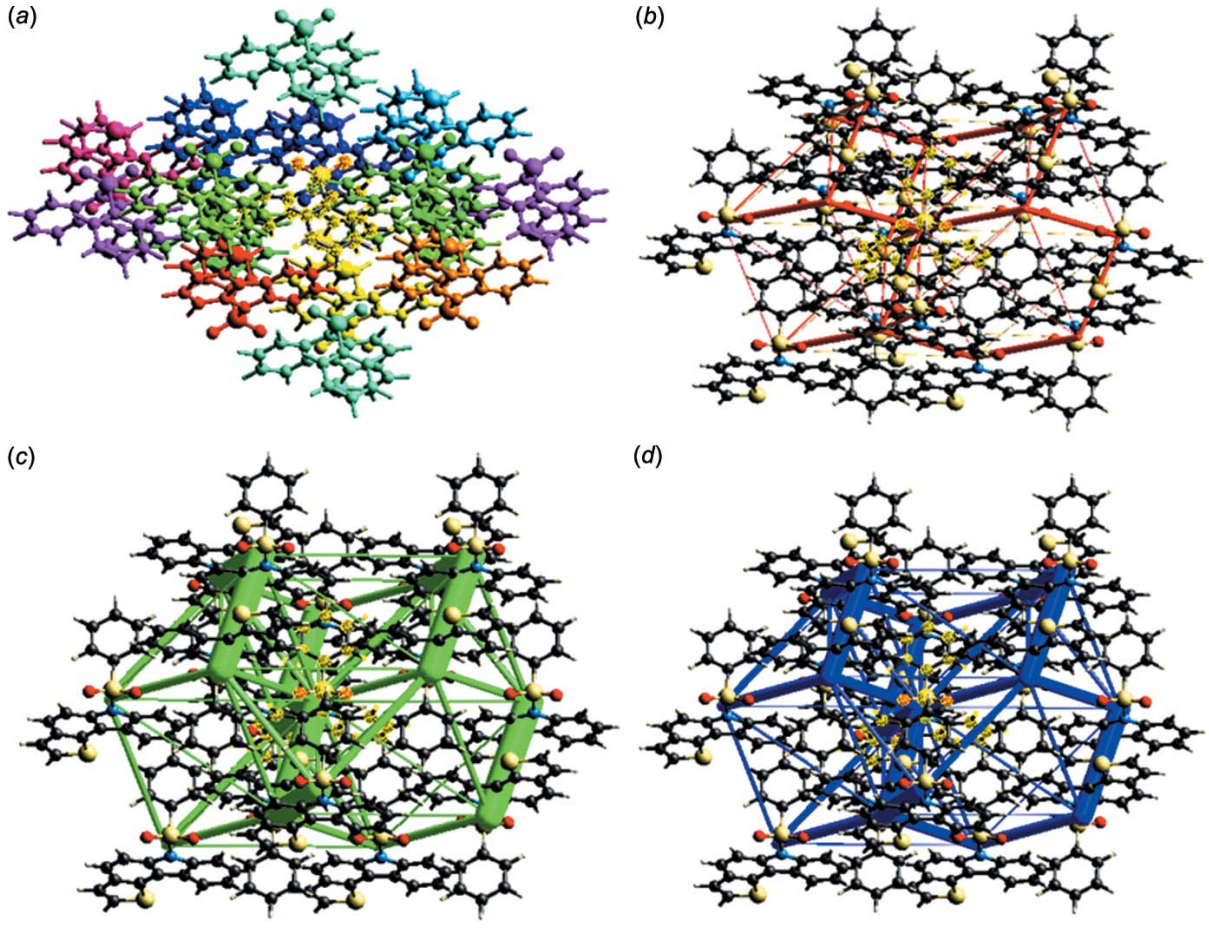

Figure 5
(*a*) Interactions between the selected reference molecule (highlighted in yellow) and the molecules present in a 3.8 Å cluster around it, (*b*) Coulomb energy framework, (*c*) dispersion energy framework and (*d*) total energy framework.

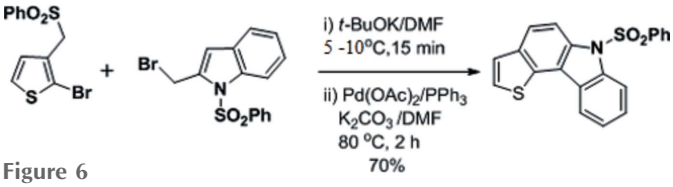

Figure 6
Reaction scheme.

marked energy model (Mackenzie *et al.*, 2017) are given in Table 2. The interaction energies calculated by the energy model reveal that the interactions in crystal have a significant contribution from dispersion components (Table 3). Using energy frameworks, the magnitudes of the intermolecular interaction energies are represented graphically and the supramolecular architecture of the crystal structure is visualized. Energies between molecular pairs are represented as cylinders joining the centroids of pairs of molecules, with the cylinder radius proportional to the magnitude of the interaction energy. Frameworks were constructed for E_{elec} as red cylinders, E_{dis} as green and E_{tot} as blue (Fig. 5*b*–5*d*) and these cylinders represent the relative strength of molecular packing in different directions.

5. Synthesis and crystallization

The first step was the alkylation of 2-bromo-3-(phenylsulfonylmethyl)thiophene (0.7 g, 2.21 mmol) with 2-bromomethyl-1-phenylsulfonylindol (0.85 g, 2.43 mmol) using *t*-BuOK (0.37 g, 3.32 mmol) in DMF (20 mL) at 278–283 K for 15 min. After completion of the reaction, the reaction mixture was poured into crushed ice. The solid obtained was filtered and dried to afford the alkylated sulfone (1.16 g) as a colourless solid. To a solution of the crude alkylated sulfone (1.16 g, 1.97 mmol) in DMF (15 mL), $Pd(OAc)_2$ (0.04 g, 0.19 mmol), PPh_3 (0.10 g, 0.39 mmol) and K_2CO_3 (0.55 g, 3.94 mmol) were added. Then the reaction mixture was heated at 353 K for 2 h. After that, the reaction mixture was filtered through a celite bed and washed with ethyl acetate (2 × 10 mL). The combined organic layer was washed with water (3 × 20 mL) and dried (Na_2SO_4). Removal of the solvent followed by column chromatographic purification (silica gel, 100% hexane) afforded 6-(phenylsulfonyl)-6*H*-thieno[3,2-*c*]carbazole (0.50 g, 70%) as a colourless solid (Fig. 6). Diffraction-quality crystals were obtained from the product by slow evaporation using chloroform as a solvent; m.p. 417–419 K.

6. Refinement

Crystal data, data collection and structure refinement details are summarized in Table 4. All H atoms were positioned geometrically (C—H = 0.93 Å) and refined using a riding model with $U_{iso}(H) = 1.2U_{eq}(C)$. In the final refinement, reflection (001), which was obstructed by the beam stop, was omitted.

Table 4
Experimental details.

Crystal data	
Chemical formula	$C_{20}H_{13}NO_2S_2$
M_r	363.43
Crystal system, space group	Triclinic, $P\overline{1}$
Temperature (K)	298
a, b, c (Å)	7.6461 (8), 9.8772 (9), 11.2191 (12)
α, β, γ (°)	72.571 (5), 88.496 (6), 86.144 (6)
V (Å^3)	806.54 (14)
Z	2
Radiation type	Mo $K\alpha$
μ (mm^{-1})	0.34
Crystal size (mm)	0.25 × 0.20 × 0.20
Data collection	
Diffractometer	Bruker Kappa APEXII CCD
Absorption correction	Multi-scan (*SADABS*; Bruker, 2012)
T_{min}, T_{max}	0.921, 0.934
No. of measured, independent and observed [$I > 2\sigma(I)$] reflections	16616, 3174, 2458
R_{int}	0.036
(sin $\theta/\lambda)_{max}$ (Å^{-1})	0.617
Refinement	
$R[F^2 > 2\sigma(F^2)]$, $wR(F^2)$, S	0.034, 0.091, 1.03
No. of reflections	3102
No. of parameters	226
H-atom treatment	H-atom parameters constrained
$\Delta\rho_{max}$, $\Delta\rho_{min}$ (e Å^{-3})	0.24, −0.41

Computer programs: *APEX2*, *SAINT* and *XPREP* (Bruker, 2012), *SHELXS97* (Sheldrick, 2008), *SHELXL2014* (Sheldrick, 2015) and *ORTEP-3 for Windows* (Farrugia, 2012).

Acknowledgements

The authors thank the Central Instrumentation Facility (DST–FIST), Queen Mary's College (A), Chennai-4 for the computing facility and SAIF, IIT, Madras, for the X-ray data-collection facility.

References

Allen, F. H., Kennard, O., Watson, D. G., Brammer, L., Orpen, A. G. & Taylor, R. (1987). *J. Chem. Soc. Perkin Trans. 2*, pp. S1–19.
Bassindale, A. (1984). *The Third Dimension in Organic Chemistry*, ch. 1, p. 11. New York: John Wiley and Sons.
Bruker (2012). *APEX2*, *SAINT*, *XPREP* and *SADABS*. Bruker AXS Inc., Madison, Wisconsin, USA.
Chakraborty, D. P., Barman, B. K. & Bose, P. K. (1965). *Tetrahedron*, **21**, 681–685.
Chakraborty, D. P., Bhattacharyya, P., Roy, S., Bhattacharyya, S. P. & Biswas, A. K. (1978). *Phytochemistry*, **17**, 834–835.
Farrugia, L. J. (2012). *J. Appl. Cryst.* **45**, 849–854.
Giraud, F., Bourhis, M., Nauton, L., Théry, V., Herfindal, L., Døskeland, S. O., Anizon, F. & Moreau, P. (2014). *Bioorg. Chem.* **57**, 108–115.
Groom, C. R., Bruno, I. J., Lightfoot, M. P. & Ward, S. C. (2016). *Acta Cryst.* B**72**, 171–179.
Gu, W., Qiao, C., Wang, S. F., Hao, Y. & Miao, T. T. (2014). *Bioorg. Med. Chem. Lett.* **24**, 328–331.
Itoigawa, M., Kashiwada, Y., Ito, C., Furukawa, H., Tachibana, Y., Bastow, K. F. & Lee, K. H. (2000). *J. Nat. Prod.* **63**, 893–897.
Jayatilaka, D., Grimwood, D. J., Lee, A., Lemay, A., Russel, A. J., Taylor, C., Wolff, S. K., Cassam-Chenai, P. & Whitton, A. (2005). *TONTO -- A System for Computational Chemistry*. Available at: http://hirshfeldsurface.net/

Karmakar, A. C., Kar, G. K. & Ray, J. K. (1991). *J. Chem. Soc. Perkin Trans. 1*, pp. 1997–2002.
Mackenzie, C. F., Spackman, P. R., Jayatilaka, D. & Spackman, M. A. (2017). *IUCrJ*, **4**, 575–587.
McKinnon, J. J., Jayatilaka, D. & Spackman, M. A. (2007). *Chem. Commun.* pp. 3814–3816.
Ramsewak, R. S., Nair, M. G., Strasburg, G. M., DeWitt, D. L. & Nitiss, J. L. (1999). *J. Agric. Food Chem.* **47**, 444–447.
Sheldrick, G. M. (2008). *Acta Cryst.* A**64**, 112–122.
Sheldrick, G. M. (2015). *Acta Cryst.* C**71**, 3–8.
Spackman, M. A., McKinnon, J. J. & Jayatilaka, D. (2008). *CrystEngComm*, **10**, 377–388.
Tachibana, Y., Kikuzaki, H., Lajis, N. H. & Nakatani, N. (2001). *J. Agric. Food Chem.* **49**, 5589–5594.
Thiratmatrakul, S., Yenjai, C., Waiwut, P., Vajragupta, O., Reubroycharoen, P., Tohda, M. & Boonyarat, C. (2014). *Eur. J. Med. Chem.* **75**, 21–30.
Turner, M. J., McKinnon, J. J., Wolff, S. K., Grimwood, D. J., Spackman, P. R., Jayatilaka, D. & Spackman, M. A. (2017). *CrystalExplorer*. The University of Western Australia.

supporting information

Acta Cryst. (2018). E**74**, 878-883 [https://doi.org/10.1107/S2056989018007971]

Crystal structure determination, Hirshfeld surface analysis and energy frameworks of 6-phenylsulfonyl-6*H*-thieno[3,2-*c*]carbazole

U. Mohamooda Sumaya, E. Sankar, K. Arasambattu MohanaKrishnan, K. Biruntha and G. Usha

Computing details

Data collection: *APEX2* (Bruker, 2012); cell refinement: *APEX2* and *SAINT* (Bruker, 2012); data reduction: *SAINT* and *XPREP* (Bruker, 2012); program(s) used to solve structure: *SHELXS97* (Sheldrick, 2008); program(s) used to refine structure: *SHELXL2014* (Sheldrick, 2015); molecular graphics: *ORTEP-3 for Windows* (Farrugia, 2012); software used to prepare material for publication: *SHELXL2014* (Sheldrick, 2015).

6-Phenylsulfonyl-6*H*-thieno[3,2-*c*]carbazole

Crystal data

$C_{20}H_{13}NO_2S_2$
$M_r = 363.43$
Triclinic, $P\overline{1}$
$a = 7.6461$ (8) Å
$b = 9.8772$ (9) Å
$c = 11.2191$ (12) Å
$\alpha = 72.571$ (5)°
$\beta = 88.496$ (6)°
$\gamma = 86.144$ (6)°
$V = 806.54$ (14) Å^3
$Z = 2$
$F(000) = 376$
$D_x = 1.497$ Mg m^{-3}
Mo $K\alpha$ radiation, $\lambda = 0.71073$ Å
Cell parameters from 3175 reflections
$\theta = 2.4$–$28.8°$
$\mu = 0.34$ mm^{-1}
$T = 298$ K
Needle, colourless
0.25 × 0.20 × 0.20 mm

Data collection

Bruker Kappa APEXII CCD diffractometer
Radiation source: fine-focus sealed tube
ω and φ scan
Absorption correction: multi-scan (SADABS; Bruker, 2012)
$T_{min} = 0.921$, $T_{max} = 0.934$
16616 measured reflections
3174 independent reflections
2458 reflections with $I > 2\sigma(I)$
$R_{int} = 0.036$
$\theta_{max} = 26.0°$, $\theta_{min} = 2.4°$
$h = -9 \rightarrow 9$
$k = -12 \rightarrow 12$
$l = -13 \rightarrow 13$

Refinement

Refinement on F^2
Least-squares matrix: full
$R[F^2 > 2\sigma(F^2)] = 0.034$
$wR(F^2) = 0.091$
$S = 1.03$
3102 reflections
226 parameters
0 restraints
Hydrogen site location: inferred from neighbouring sites
H-atom parameters constrained
$w = 1/[\sigma^2(F_o^2) + (0.0389P)^2 + 0.3787P]$ where $P = (F_o^2 + 2F_c^2)/3$
$(\Delta/\sigma)_{max} < 0.001$
$\Delta\rho_{max} = 0.24$ e Å^{-3}
$\Delta\rho_{min} = -0.41$ e Å^{-3}

Special details

Geometry. All esds (except the esd in the dihedral angle between two l.s. planes) are estimated using the full covariance matrix. The cell esds are taken into account individually in the estimation of esds in distances, angles and torsion angles; correlations between esds in cell parameters are only used when they are defined by crystal symmetry. An approximate (isotropic) treatment of cell esds is used for estimating esds involving l.s. planes.

Fractional atomic coordinates and isotropic or equivalent isotropic displacement parameters (Å²)

	x	*y*	*z*	U_{iso}*/U_{eq}
C1	0.3947 (3)	0.2820 (2)	0.4004 (2)	0.0462 (5)
H1	0.4480	0.1960	0.4478	0.055*
C2	0.3350 (4)	0.3854 (3)	0.4540 (2)	0.0590 (7)
H2	0.3496	0.3685	0.5394	0.071*
C3	0.2541 (4)	0.5137 (3)	0.3848 (2)	0.0614 (7)
H3	0.2148	0.5806	0.4242	0.074*
C4	0.2317 (3)	0.5426 (2)	0.2583 (2)	0.0478 (6)
H4	0.1776	0.6287	0.2118	0.057*
C5	0.2909 (3)	0.44110 (19)	0.20083 (18)	0.0327 (4)
C6	0.3716 (3)	0.31203 (19)	0.27287 (18)	0.0331 (4)
C7	0.3683 (2)	0.30993 (19)	0.06791 (17)	0.0313 (4)
C8	0.2892 (2)	0.43910 (19)	0.07345 (17)	0.0300 (4)
C9	0.3877 (3)	0.2747 (2)	−0.04358 (19)	0.0395 (5)
H9	0.4417	0.1880	−0.0450	0.047*
C10	0.3247 (3)	0.3722 (2)	−0.1510 (2)	0.0432 (5)
H10	0.3350	0.3499	−0.2259	0.052*
C11	0.2454 (3)	0.5042 (2)	−0.15089 (19)	0.0378 (5)
C12	0.2289 (2)	0.53705 (19)	−0.03801 (19)	0.0335 (4)
C13	0.1126 (3)	0.7312 (2)	−0.2176 (2)	0.0526 (6)
H13	0.0633	0.8143	−0.2728	0.063*
C14	0.1762 (3)	0.6197 (2)	−0.2532 (2)	0.0499 (6)
H14	0.1756	0.6172	−0.3354	0.060*
C15	0.2718 (3)	−0.02095 (18)	0.26426 (18)	0.0318 (4)
C16	0.2018 (3)	−0.0612 (2)	0.38416 (19)	0.0392 (5)
H16	0.2624	−0.0493	0.4508	0.047*
C17	0.0401 (3)	−0.1193 (2)	0.4027 (2)	0.0458 (5)
H17	−0.0082	−0.1480	0.4826	0.055*
C18	−0.0494 (3)	−0.1347 (2)	0.3035 (2)	0.0482 (6)
H18	−0.1589	−0.1727	0.3166	0.058*
C19	0.0212 (3)	−0.0946 (2)	0.1843 (2)	0.0473 (5)
H19	−0.0408	−0.1052	0.1178	0.057*
C20	0.1835 (3)	−0.0388 (2)	0.1641 (2)	0.0405 (5)
H20	0.2332	−0.0135	0.0845	0.049*
O1	0.55980 (19)	0.02188 (14)	0.13545 (14)	0.0426 (4)
O2	0.56255 (19)	0.02622 (14)	0.35412 (13)	0.0423 (4)
S1	0.13085 (7)	0.70590 (5)	−0.05968 (6)	0.04557 (17)
S2	0.47505 (6)	0.05704 (5)	0.23770 (5)	0.03323 (14)
N1	0.4252 (2)	0.23071 (16)	0.19079 (14)	0.0332 (4)

Atomic displacement parameters (Å²)

	U^{11}	U^{22}	U^{33}	U^{12}	U^{13}	U^{23}
C1	0.0662 (15)	0.0380 (12)	0.0332 (12)	−0.0017 (10)	−0.0041 (11)	−0.0091 (9)
C2	0.094 (2)	0.0533 (14)	0.0340 (12)	−0.0060 (13)	0.0035 (13)	−0.0189 (11)
C3	0.095 (2)	0.0454 (14)	0.0500 (15)	−0.0002 (13)	0.0092 (14)	−0.0256 (12)
C4	0.0623 (15)	0.0344 (11)	0.0468 (13)	0.0051 (10)	0.0037 (11)	−0.0143 (10)
C5	0.0353 (11)	0.0284 (9)	0.0352 (11)	−0.0037 (8)	0.0016 (8)	−0.0105 (8)
C6	0.0376 (11)	0.0299 (10)	0.0331 (10)	−0.0034 (8)	0.0006 (8)	−0.0111 (8)
C7	0.0332 (10)	0.0278 (9)	0.0313 (10)	−0.0025 (7)	−0.0018 (8)	−0.0060 (8)
C8	0.0289 (10)	0.0267 (9)	0.0345 (10)	−0.0039 (7)	0.0000 (8)	−0.0091 (8)
C9	0.0520 (13)	0.0321 (10)	0.0361 (11)	0.0008 (9)	0.0007 (10)	−0.0138 (9)
C10	0.0570 (14)	0.0434 (12)	0.0312 (11)	−0.0052 (10)	−0.0007 (10)	−0.0138 (9)
C11	0.0395 (12)	0.0363 (11)	0.0349 (11)	−0.0065 (9)	−0.0049 (9)	−0.0053 (9)
C12	0.0315 (10)	0.0274 (9)	0.0394 (11)	−0.0043 (8)	−0.0022 (8)	−0.0057 (8)
C13	0.0534 (15)	0.0415 (13)	0.0508 (14)	0.0009 (10)	−0.0151 (11)	0.0051 (11)
C14	0.0554 (15)	0.0509 (14)	0.0369 (12)	−0.0075 (11)	−0.0106 (11)	−0.0012 (10)
C15	0.0354 (11)	0.0243 (9)	0.0354 (11)	0.0050 (7)	−0.0050 (8)	−0.0095 (8)
C16	0.0436 (12)	0.0368 (11)	0.0365 (11)	0.0035 (9)	−0.0044 (9)	−0.0111 (9)
C17	0.0472 (13)	0.0432 (12)	0.0455 (13)	−0.0025 (10)	0.0070 (11)	−0.0116 (10)
C18	0.0366 (12)	0.0391 (12)	0.0694 (16)	−0.0011 (9)	0.0007 (11)	−0.0173 (11)
C19	0.0470 (13)	0.0443 (12)	0.0546 (14)	−0.0018 (10)	−0.0144 (11)	−0.0199 (11)
C20	0.0470 (13)	0.0366 (11)	0.0373 (11)	0.0013 (9)	−0.0045 (10)	−0.0106 (9)
O1	0.0446 (9)	0.0362 (8)	0.0472 (9)	0.0064 (6)	0.0048 (7)	−0.0150 (6)
O2	0.0417 (8)	0.0387 (8)	0.0427 (9)	0.0048 (6)	−0.0145 (7)	−0.0066 (6)
S1	0.0462 (3)	0.0317 (3)	0.0526 (4)	0.0048 (2)	−0.0053 (3)	−0.0043 (2)
S2	0.0342 (3)	0.0271 (2)	0.0365 (3)	0.00447 (18)	−0.0042 (2)	−0.0077 (2)
N1	0.0429 (10)	0.0271 (8)	0.0287 (8)	0.0026 (7)	−0.0039 (7)	−0.0077 (7)

Geometric parameters (Å, º)

C1—C2	1.380 (3)	C11—C14	1.437 (3)
C1—C6	1.385 (3)	C12—S1	1.7323 (19)
C1—H1	0.9300	C13—C14	1.338 (3)
C2—C3	1.386 (4)	C13—S1	1.722 (3)
C2—H2	0.9300	C13—H13	0.9300
C3—C4	1.374 (3)	C14—H14	0.9300
C3—H3	0.9300	C15—C20	1.387 (3)
C4—C5	1.392 (3)	C15—C16	1.387 (3)
C4—H4	0.9300	C15—S2	1.760 (2)
C5—C6	1.401 (3)	C16—C17	1.382 (3)
C5—C8	1.435 (3)	C16—H16	0.9300
C6—N1	1.428 (2)	C17—C18	1.374 (3)
C7—C8	1.392 (3)	C17—H17	0.9300
C7—C9	1.397 (3)	C18—C19	1.382 (3)
C7—N1	1.429 (2)	C18—H18	0.9300
C8—C12	1.399 (3)	C19—C20	1.378 (3)
C9—C10	1.373 (3)	C19—H19	0.9300

C9—H9	0.9300	C20—H20	0.9300
C10—C11	1.401 (3)	O1—S2	1.4233 (15)
C10—H10	0.9300	O2—S2	1.4236 (15)
C11—C12	1.399 (3)	S2—N1	1.6572 (16)

C2—C1—C6	117.0 (2)	C8—C12—S1	128.08 (16)
C2—C1—H1	121.5	C14—C13—S1	113.43 (17)
C6—C1—H1	121.5	C14—C13—H13	123.3
C1—C2—C3	122.1 (2)	S1—C13—H13	123.3
C1—C2—H2	118.9	C13—C14—C11	112.8 (2)
C3—C2—H2	118.9	C13—C14—H14	123.6
C4—C3—C2	120.5 (2)	C11—C14—H14	123.6
C4—C3—H3	119.8	C20—C15—C16	121.34 (19)
C2—C3—H3	119.8	C20—C15—S2	119.11 (16)
C3—C4—C5	119.1 (2)	C16—C15—S2	119.55 (16)
C3—C4—H4	120.5	C17—C16—C15	118.7 (2)
C5—C4—H4	120.5	C17—C16—H16	120.6
C4—C5—C6	119.44 (19)	C15—C16—H16	120.6
C4—C5—C8	132.60 (19)	C18—C17—C16	120.2 (2)
C6—C5—C8	107.96 (16)	C18—C17—H17	119.9
C1—C6—C5	121.89 (18)	C16—C17—H17	119.9
C1—C6—N1	130.16 (18)	C17—C18—C19	120.8 (2)
C5—C6—N1	107.91 (17)	C17—C18—H18	119.6
C8—C7—C9	122.62 (18)	C19—C18—H18	119.6
C8—C7—N1	108.02 (16)	C20—C19—C18	120.0 (2)
C9—C7—N1	129.33 (17)	C20—C19—H19	120.0
C7—C8—C12	118.03 (17)	C18—C19—H19	120.0
C7—C8—C5	108.38 (16)	C19—C20—C15	119.0 (2)
C12—C8—C5	133.58 (18)	C19—C20—H20	120.5
C10—C9—C7	117.95 (19)	C15—C20—H20	120.5
C10—C9—H9	121.0	C13—S1—C12	91.09 (11)
C7—C9—H9	121.0	O1—S2—O2	120.14 (9)
C9—C10—C11	121.76 (19)	O1—S2—N1	106.94 (8)
C9—C10—H10	119.1	O2—S2—N1	106.82 (8)
C11—C10—H10	119.1	O1—S2—C15	108.46 (9)
C12—C11—C10	119.05 (18)	O2—S2—C15	108.51 (9)
C12—C11—C14	111.32 (19)	N1—S2—C15	104.96 (9)
C10—C11—C14	129.6 (2)	C6—N1—C7	107.66 (15)
C11—C12—C8	120.57 (18)	C6—N1—S2	124.02 (13)
C11—C12—S1	111.34 (15)	C7—N1—S2	124.80 (13)

C6—C1—C2—C3	0.5 (4)	C12—C11—C14—C13	0.1 (3)
C1—C2—C3—C4	−0.5 (4)	C10—C11—C14—C13	−178.9 (2)
C2—C3—C4—C5	0.2 (4)	C20—C15—C16—C17	−0.4 (3)
C3—C4—C5—C6	0.1 (3)	S2—C15—C16—C17	178.53 (15)
C3—C4—C5—C8	−179.2 (2)	C15—C16—C17—C18	−0.8 (3)
C2—C1—C6—C5	−0.2 (3)	C16—C17—C18—C19	0.9 (3)
C2—C1—C6—N1	176.9 (2)	C17—C18—C19—C20	0.2 (3)

C4—C5—C6—C1	−0.1 (3)	C18—C19—C20—C15	−1.4 (3)
C8—C5—C6—C1	179.39 (19)	C16—C15—C20—C19	1.6 (3)
C4—C5—C6—N1	−177.79 (18)	S2—C15—C20—C19	−177.40 (15)
C8—C5—C6—N1	1.7 (2)	C14—C13—S1—C12	0.00 (19)
C9—C7—C8—C12	−0.6 (3)	C11—C12—S1—C13	0.04 (16)
N1—C7—C8—C12	177.62 (16)	C8—C12—S1—C13	179.58 (19)
C9—C7—C8—C5	−179.87 (18)	C20—C15—S2—O1	−30.91 (17)
N1—C7—C8—C5	−1.6 (2)	C16—C15—S2—O1	150.12 (15)
C4—C5—C8—C7	179.3 (2)	C20—C15—S2—O2	−162.97 (15)
C6—C5—C8—C7	0.0 (2)	C16—C15—S2—O2	18.06 (18)
C4—C5—C8—C12	0.2 (4)	C20—C15—S2—N1	83.12 (16)
C6—C5—C8—C12	−179.1 (2)	C16—C15—S2—N1	−95.86 (16)
C8—C7—C9—C10	−0.4 (3)	C1—C6—N1—C7	179.9 (2)
N1—C7—C9—C10	−178.23 (19)	C5—C6—N1—C7	−2.7 (2)
C7—C9—C10—C11	0.9 (3)	C1—C6—N1—S2	20.2 (3)
C9—C10—C11—C12	−0.5 (3)	C5—C6—N1—S2	−162.32 (14)
C9—C10—C11—C14	178.4 (2)	C8—C7—N1—C6	2.7 (2)
C10—C11—C12—C8	−0.6 (3)	C9—C7—N1—C6	−179.27 (19)
C14—C11—C12—C8	−179.65 (18)	C8—C7—N1—S2	162.11 (14)
C10—C11—C12—S1	179.00 (16)	C9—C7—N1—S2	−19.8 (3)
C14—C11—C12—S1	−0.1 (2)	O1—S2—N1—C6	−166.71 (15)
C7—C8—C12—C11	1.1 (3)	O2—S2—N1—C6	−36.89 (18)
C5—C8—C12—C11	−179.87 (19)	C15—S2—N1—C6	78.21 (17)
C7—C8—C12—S1	−178.41 (14)	O1—S2—N1—C7	37.08 (18)
C5—C8—C12—S1	0.6 (3)	O2—S2—N1—C7	166.91 (15)
S1—C13—C14—C11	0.0 (3)	C15—S2—N1—C7	−78.00 (17)

Hydrogen-bond geometry (Å, º)

Cg5 is the centroid of the C15–C20 ring.

D—H···*A*	*D*—H	H···*A*	*D*···*A*	*D*—H···*A*
C1—H1···O2	0.93	2.34	2.935 (3)	121
C1—H1···O2^{i}	0.93	2.62	3.443 (3)	148
C9—H9···O1	0.93	2.35	2.949 (3)	122
C9—H9···O1^{ii}	0.93	2.57	3.382 (2)	146
C13—H13···*Cg*5^{iii}	0.93	2.82	3.604 (2)	143

Symmetry codes: (i) −*x*+1, −*y*, −*z*+1; (ii) −*x*+1, −*y*, −*z*; (iii) −*x*, −*y*+1, −*z*.